Published in final edited form as:
J Immunol. 2010 December 15; 185(12): 7544–7552. doi:10.4049/jimmunol.1002665.

The Igκ Gene Enhancers, E3′ and Ed, Are Essential for Triggering Transcription

Xiaorong Zhou[*,‡], **Yougui Xiang**[*], and **William T. Garrard**[*,2]

[*]Department of Molecular Biology, University of Texas Southwestern Medical Center, 5323 Harry Hines Blvd., Dallas, TX 75390-9148

[‡]Department of Microbiology and Immunology, Medical School of Nantong University, 19 Qixiu Road, Nantong, Jiangsu 226001, PR China

Abstract

The mouse Igκ gene locus has three known transcriptional enhancers: an intronic enhancer (Ei), a 3′ enhancer (E3′), and a further downstream enhancer (Ed). Previous studies on B lymphocytes derived from mutant ES cells have shown that deletion of either Ei or E3′ significantly reduces Igκ gene rearrangement, whereas the combined deletion of both Ei and E3′ eliminates such recombination. Furthermore, deletion of either E3′ or Ed significantly reduces rearranged Igκ gene transcription. To determine whether the combined presence of both E3′ and Ed are essential for Igκ gene expression, we generated homozygous double knockout mice (DKO) with targeted deletions in both elements. Significantly, homozygous DKO mice were unable to generate κ^+ B cells both in bone marrow and the periphery, and exhibited surface expression almost exclusively of Igλ chains, in spite of the fact that they possessed potentially functional rearranged Igκ genes. Compared with their single-enhancer-deleted counterparts, Igκ loci in homozygous DKO mice exhibited dramatically reduced germline and rearranged gene transcription, lower levels of gene rearrangement and histone H3 acetylation, and markedly increased DNA methylation. This contributed to a partial developmental block at the pre-B cell stage of development. We conclude that the two downstream enhancers are essential in Igκ gene expression and that Ei in homozygous DKO mice is incapable of triggering Igκ gene transcription. Furthermore, these results reveal unexpected compensatory roles for Ed in E3′ knockout mice in triggering germline transcription, and Vκ gene rearrangements to both Jκ and RS elements.

Keywords

B cells; gene regulation; knockout mice; enhancers; transcription; gene rearrangement

Introduction

During B cell development the IgH gene locus functionally rearranges first, by V(D)J joining events, leading to the pre-B cell stage of differentiation (1). Next, the Igκ locus is poised for rearrangement, and upon appropriate signaling one of the 96 potentially functional Vκ genes is semi-randomly selected for recombination to a Jκ region (2; for reviews, see refs. 3,4). If Igκ gene rearrangement is productively unsuccessful because of

[2]Address correspondence and reprint requests to Dr. William T. Garrard, Department of Molecular Biology, University of Texas Southwestern Medical Center, 5323 Harry Hines Blvd., Dallas, TX 75390-9148. Phone: 214-648-1924. FAX: 214-648-1915. william.garrard@utsouthwestern.edu.

None of the authors have any financial interest related to this work.

out-of-reading frame recombination junctions, then the Igλ locus becomes activated for rearrangement and expression, which in wild type mice normally accounts for production of less than 5% of the total IgL chains. Interestingly, most λ–producing B cells possess aberrantly rearranged and deleted Igκ genes because of Vκ joining to a recombining sequence (RS)[3] near the 3′-end of the locus (5–8).

Research in our laboratory has focused on the Igκ locus, because it offers the opportunity to visualize changes in chromatin structure that may precede gene rearrangement and transcriptional activation during B lymphocyte differentiation, as well as those remodeling events that may accompany or be a consequence of gene activation (9 and refs. within). Rearrangement of the Igκ locus results in its transcriptional activation because it positions a Vκ gene carrying its own promoter into a chromatin domain containing three powerful enhancers: an intronic enhancer (Ei) within the transcription unit (10), and two enhancers downstream of the transcription termination region (11), termed E3′ (12) and Ed (9). Experimental evidence supports the proposal that these enhancers mediate transcriptional activation via a regulated looping mechanism. In activated B cells, the three enhancers exhibit all possible pair-wise interactions with each other and with rearranged Vκ gene promoters, with the looping out of the intervening DNA sequences (13). However, in unstimulated B cells, rearranged Vκ gene promoters only form complexes with either Ei or E3′, but not with Ed, with the looping out of the intervening DNA, resulting in a transcriptionally poised state in the locus (14).

Previous studies have determined the functional significance of Ei, E3′ and Ed in Igκ gene dynamics in B lymphocytes by first creating individual targeted deletions of each. These experiments revealed that Ei and E3′ each play quantitative but not essential roles in gene rearrangement (15,16), while E3′ and Ed each play quantitative but not essential roles in rearranged gene transcription (16,17). Ed, the farthest downstream enhancer residing some 8 kb away from E3′, plays no role in gene rearrangement and maximally acts during the latest stages of B cell differentiation (17). Indeed, a double deletion of both Ei and E3′ proves to eliminate Igκ gene rearrangement (18). In the current investigation we explore whether the combined presence of both E3′ and Ed are essential for triggering rearranged gene transcription and other events linked to expression of the Igκ gene locus. For this purpose we created homozygous double knockout (DKO) mice with germline targeted deletions in both E3′ and Ed using state-of-the-art BAC recombineering technology. Our results reveal a severe downregulation in rearranged Igκ gene expression. Unexpectedly, our results also allow us to deduce that Ed must play compensatory roles in E3′ knockout mice for triggering germline transcription, and Vκ gene rearrangements to both Jκ and RS elements.

Materials and Methods

Generation of DKO mice

We utilized BAC recombineering technology (19,20) with modifications to generate an ES cell targeting construct for creating DKO mice. The bacterial strains and plasmids utilized were provided by researchers at NCI-Frederick (http://web.ncifcrf.gov/research/brb/reagents/recombineeringReagent.aspx). BAC clone (BMQ-62L21) carrying the relevant 3′ region of the mouse SV129 Igκ locus (Geneservice) was electroporated into *E. coli* strain SW102, which harbors a defective λ prophage encoding the *exo*, *bet*, and *gam* genes under the control of the temperature-sensitive repressor *cI*857. E3′ was amplified by PCR with primers in which two loxP sites were introduced at the same nucleotide positions to those present in the previously created E3′ knockout mice (16), along with added I-*Sce*I, *Eco*RI and *Nhe*I sites for subcloning into plasmid pL452, which carries a *Neo* gene. Overlapping PCR was then performed to combine 250 bp H2 and H3 homologous arms (prepared by PCR amplification from the BAC)(Fig.

1*Aa*). The resulting product was blunt-end subcloned into the pSC-B-amp^{r}/kan^{r} plasmid (Agilent Technologies, Inc.). After the desired structure was confirmed by sequencing, the excised *Eco*RI fragment was integrated into the BAC carrying strain, which had been induced for recombination functions by prior heat-shock at 42°C for 15 min. Resulting kanamycin resistant clones were screened by PCR to confirm that the cassette had correctly integrated into the BAC. For targeting Ed, PCR and subcloning steps were performed similar to those described above to flank a *Puro* gene with two frt sites, one I-*Sce*I site, and 250 bp homologous arms H4 and H5 in the plasmid pSELECT-puro/mcs (InvivoGen)(Fig. 1*Ab*), recreating the identical nucleotide deletion of Ed knockout mice (17). The purified *Puro* cassette was used to transform the heat-shocked BAC-carrying strain to kanamycin and puromycin resistance. The functionality of the targeted loxP and frt sites in the engineered BAC were tested by introduction into SW105 (Flp^{+}) and SW106 (Cre^{+}) *E. coli* strains. For DNA retrieval of the targeting module, two 50 bp homologous sequences H1 and H6 with added *Not*I sites were used to amplify plasmid pL611 and PCR products were introduced into heat-shocked *E. coli* carrying the engineered BAC by electroporation (Fig. 1*B*). Resulting Amp resistant plasmids carrying the 26 kb DKO targeting vector were confirmed by sequencing. The SM-1 (129/SvEvTac) ES cell line was transformed by electroporation with the *Not*I plasmid-free fragment. G418 and puromycin double-resistant ES cell clones were first screened by PCR and correctly targeted clones were then verified by Southern blotting. External probes for Southern blots were amplified from the BAC by high fidelity PCR (Supplemental Fig. S1). Further details of the above procedures will be made available upon request. Three independent targeted clones were injected into C57/BL6 blastocysts. Resulting chimeric mice were bred with C57/BL6 mice to obtain germline transmission. To obtain DKO mice, germline transmissible mice were bred with intercrossed Cre and Flp recombinase expressing mice (21,22). All mice were used in accordance with protocols approved by the UT Southwestern Medical Center Institutional Animal Care and Use Committee (IACUC).

Other mouse strains

E3′−/− mice, originally produced by Fred Alt's laboratory (16), were kindly provided by Mark Schlissel. Ed−/− mice were previously established in our laboratory (17).

Flow cytometry and cell fractionations

Single-cell suspensions were prepared from bone marrow and spleens of 6–12 week old mice. Cellular populations were analyzed using FACS Calibur with CellQuest software (BD Bioscence) or FlowJo software (Tree Star). Antibodies used from BD Bioscience were anti-B220-FITC, anti-mouse-Igκ-PE, anti-mouse-CD25-PE, anti-Igλ1,2,3-FITC, and anti-mouse-CD43-PE; anti-IgM-FITC was purchased from Southern Biotech. Splenic B cells were isolated by biotinylated anti-B220 antibody using MACS MS columns (Miltenyi Biotech). Pre-B cells (CD19^{+}CD25^{+}IgM^{-}) were sorted from bone marrow using a Moflo machine (Dako cytomation).

Analysis of Igκ gene rearrangement

Pre-B and splenic B cells purified as described above were lysed in lysis buffer with proteinase K. Genomic DNA was then purified by phenol/chloroform extraction, followed by ethanol precipitation. Vκ-Jκ rearrangement products were PCR amplified using a degenerate Vκ primer (VκD) (23) and a Mar35 primer (18). PCR primers used here and elsewhere are listed in Table I. The amount of genomic DNA used in each PCR reaction was adjusted so that the products would be roughly proportional to template concentration based on the output signal of β-actin gene PCR reactions, and PCR products were resolved by electrophoresis in 1% agarose gels.

VκD-Jκ1 rearrangement products and the germline retention of Igκ alleles were determined by real-time PCR assays, using either forward and reverse primers that were complementary to VκD and sequences downstream of J1 (J1-2R), or using forward and reverse primers that were complementary to sequences upstream (KGL-F) and downstream of Jκ1 (KGL-R), as described previously (24). Germline levels were normalized to the levels of an β-actin genomic region. The percentage of Igκ germline alleles was calculated by dividing the corresponding levels in WT or knockout mice B cells by those in ES cells.

For Southern blotting to quantitate germline sequences using modifications of published techniques (16,17), the membranes were hybridized with a probe obtained by cutting the Igκ containing plasmid Psp1g8 with *Sac*I and *Sac*II (constructed in our laboratory). The c-myb probe was prepared by PCR using primers, 5′-GTATGTCTAGAGTTGTCACGACA-3′ and 5′-TTCCAGATCTTTCTACCTCCACT-3′. Hybridized membranes were exposed to PhosphorImaging screens, and images were analyzed using ImageQuant software (Molecular Dynamics).

To analyze RS rearrangements, $B220^{+}Ig\lambda^{+}$ B cells were sorted from splenocytes, and genomic DNA was purified. Real-time PCR then was performed with a degenerate Vκ primer (VκD) and a RS101 primer (25)(Table I). Relative rearrangements were calculated using the ΔC_t method according to the manufacturer's instructions and normalized to an β-actin genomic region.

Real-time PCR for germline transcription and expression of Igκ

To examine Igκ gene germline transcription (KGT), total RNA, extracted from 5×10^5 purified pre-B cells using Trizol reagent (Invitrogen), was reverse transcribed into cDNA with The SuperScript VILO cDNA Synthesis Kit (Invitrogen). Real-time PCR was performed with KGT-F and KGT-R primers (Table I). The levels of Igκ gene mRNA were examined by real-time PCR with VκD and Cκ primers. Transcript levels were calculated using the ΔC_t method according to the manufacturer's instructions and normalized to the cDNA levels of the mouse hypoxanthine-guanine phosphoribosyltransferase (HPRT) gene.

Methylation analysis by bisulfite sequencing

Genomic DNA from pre-B cells and $B220^{+}$ splenic cells were converted with sodium bisulfite using the EpiTect bisulfite kit (Qiagen). For pre-B cells methylation status analysis, bisulfite converted pre-B DNA was used to amplify 3′ germline and Jκ1 region by using Platum highfidelty Taq polymerase (Invitrogen). The primers are: 5′-TTTGTAGTTGGAGTAATAGATAGT-3′ and 5′-TTAAACATAAAAACCACAAACATA-3′. For splenic B cells methylation status analysis, bisulfite converted DNA from splenic $B220^{+}$ cells was used to amplify sequences between Jκ5 and Ei enhancer. The primers are: 5′-GATGTGGGAGTAAATTTTGAAGATAAATTG-3′ and 5′-ACACCTCTTCTAATCATTCAACAAACCATA-3′. PCR program is: 94°C 3 min followed 35 cycles of 94°C 30s, 56°C 30s, 68°C 30s, and followed 68°C 5 min final extension. PCR products were agarose gel purified and cloned into PGEM-Teasy vector (Promega). Clones with inserted PCR fragment were sent to sequencing by using T7 primer. Methylation statuses of sequences were analyzed using the Vector NTI AlignX program (Invitrogen).

Chromatin IP (ChIP) assays

ChIP assays on isolated pre-B cells were performed as described previously (13). Approximately 2×10^6 cells suspended in PBS were crosslinked by adding formaldehyde to a final concentration of 1% for 10 min at 37°C. Antibodies against acetylated histone H3 were purchased from Millipore (06–599). ChIPs were performed according to Millipore's

protocol. Results were quantitated by real-time PCR with SYBR Green dye using the ABI Prism 7300 system. All PCR signals from IP samples were referenced to their respective inputs to normalize for differences in primer efficiencies. GAPDH was treated as a negative control and its enrichment fold was considered as 1. The enrichment of every test fragment was referenced to GAPDH. The real-time PCR assays were repeated two to three times and were averaged. Primers used are as reported elsewhere (26).

Results

Generation of E3′−/− Ed−/− double knockout (DKO) mice

We separately targeted both E3′ and Ed in a BAC by homologous recombination in *E. coli* for the eventual creation of DKO mice. E3′ was targeted first by introducing loxP sites flanking it and a *Neo* gene (Fig. 1*Aa*). This was followed next by inserting a *Puro* gene with flanking frt sites in place of Ed (Fig. 1*Ab*). The relevant region of the engineered BAC for ES cell targeting was then retrieved by the plasmid rescue technique, and excised by *Not*I cleavage for isolation and subsequent electroporation into ES cells (Fig. 1*B*). Several ES cell clones that exhibited site-directed integration were obtained after screening by PCR and Southern blotting. Three independent targeted ES cell clones were used to generate chimeric mice lines, which were bred with C57/BL6 mice to obtain germline transmission. Southern blotting of tail DNA confirmed that the targeting construct had appropriately replaced the endogenous sequences in the mouse germline; for example, cleavage with *Spe*I+*Nhe*I, I-*Sce*I, or *Hind*III and probing with external- or internal-specific Igκ sequences revealed the correct predicted DNA configurations (Supplemental Fig. S1). Finally, to delete E3′, along with the *Neo* and *Puro* genes (Fig. 1*D*), we bred the germline transmissible mice with Cre and Flp recombinase expressing mice (21,22). This resulted in the presence of single loxP and frt sites in place of E3′ and Ed, respectively (Fig. 1*D*, triangles). The correct structures for the DKO alleles were confirmed by Southern blotting of tail DNA samples, using probes A and B after *Bam*H1 digestion, as shown in Fig. 1*C*, *D*, and *E*).

DKO mice exhibit dramatic decreases in cell surface expression of Igκ chains in bone marrow and splenic B cells, and marked increases in cell surface expression of Igλ chains

To evaluate the effects of the DKO on B cell populations expressing surface Igκ chains, we compared the FACS patterns of B cells from spleen and bone marrow of these homozygous mice with those derived from WT mice as well as those carrying homozygous deletions of either E3′ or Ed alone (designated throughout as E3′−/− and Ed−/− mice, respectively. As shown in Fig. 2*A*, E3′−/− and Ed−/− mice exhibited significant reductions in B cell populations expressing surface Igκ chains relative to those exhibited by WT mice, in both spleen and bone marrow, in general agreement with previously published results (16,17). Notably, however, the DKO mice exhibited dramatically more severe defects in cell surface expression of Igκ chains, with such B cell populations essentially being absent from both spleen and bone marrow (Fig. 2*A*). Also in agreement with previously published results (16,17), the percentages of $Ig\lambda^+$ B cells was increased up to several fold in either E3′−/− or Ed−/− mice spleen as compared to the levels observed in WT mice (Fig. 2*B*). Particularly striking, however, was the almost exclusive high-level appearance of splenic B cells expressing Igλ chains in the DKO mice (Fig. 2*B*). We conclude that in the homozygous single enhancer knockout mice, Ed must compensate for E3′ and *visa versa* in Igκ gene expression, and that when both of these enhancers are missing, Igκ gene expression is essentially eliminated, with the expression of Igλ chains dominating. In addition, we found that the total number of $B220^+$ cells in spleen of young adult DKO mice was reduced from $4.1\pm1.3\times10^7$ cells seen in WT mice to $1.4\pm0.3\times10^7$ cells in DKO mice, a value about 34% of the level of WT animals (n=6, $p<0.01$, Supplemental Table S1), which by comparison is more severe than the 47% of WT level reported in E3′−/− animals (16). However, the total

number of $B220^+$ cells in bone marrow of young adult DKO mice was not significantly different from the values observed in WT mice (n=5, p=0.95, Supplemental Table S1). Finally, when we repeated these experiments to evaluate cell surface Igκ and Igλ expression in spleen and bone marrow of E3′+Ed+/ E3′−Ed− heterozygotes, we found that Igλ expression was greatly diminished in spleen and that cells expressing Igκ chains dominated, indicating that the haploid WT Igκ allele was capable of largely compensating for its inactivated partner (n=4, p<0.05 vs WT or DKO, Supplemental Table S1).

Early B cell development is retarded in DKO mice at the pre-B cell stage

To determine the consequences of the DKO on early B cell development, we compared the pre-B cell populations in the bone marrow of these mice with those of WT, E3′−/−, and Ed −/− mice. Two different approaches are commonly used to visualize or isolate mouse pre-B cells by FACS, based on their expression of surface markers: the Rolink et al. (27) procedure, which defines pre-B cells as $B220^+CD25^+IgM^-$, and the Hardy et al. (28) procedure, which defines pre-B cells as $B220^+CD43^-IgM^-$. We have utilized the Rolink et al. (27) procedure throughout the present investigation, which has also been used recently and gained popularity among other investigators (29,30). As shown in Fig. 3*A*, E3′−/− but not Ed−/− mice exhibited small but significant increases in pre-B cells relative to the levels exhibited by WT mice. However, the DKO mice exhibited much more dramatic increases in pre-B cells in their bone marrow (Fig. 3*A*), which we estimate is approximately a 2.6-fold increase over WT (n=4, p<0.05, Supplemental Table S1). To analyze the pro-B cell populations, bone marrow cells were gated on IgM^-, $B220^{low}$ B cells (Fig. 3*B*, rectangles), and then characterized for CD43 expression. As shown in Fig. 3*C*, within this gated population the percentage of $CD43^+$, IgM^-, $B220^{low}$ pro-B cells was dramatically reduced in DKO mice compared to those exhibited by mice of the other genetic backgrounds (Fig. 3*C*, horizontal bars); the vast majority of $B220^{low}IgM^-$ cells were $CD43^-$ pre-B cells in DKO mice. This was a consequence of the increased total numbers of pre-B cells within this gated population. Thus, the total number of pro-B cells was nearly constant. We conclude that the effects of the DKO mutations with respect to early B-cell development are to retard pre-B cell maturation in the bone marrow compartment.

The DKO decreases Igκ locus gene rearrangement beyond that observed by single enhancer deletions

In view of the lack of Igκ gene expression in DKO mice, we first examined the effect that this double deletion had on Igκ locus gene rearrangement (Fig. 4). Using PCR, we assayed for the relative usage of Jκ1–4 regions in splenic B cells using a degenerate VκD primer and the Mar35 primer (Fig. 4*A* and *B*). We found that each of the four Jκ regions were functional in Vκ-Jκ joining in either E3′−/− or Ed−/− mice like WT controls, as well as in those from DKO mice. However, the levels of Vκ-Jκ joining were most severely reduced in the DKO mice samples (Fig. 4*B*). To more accurately quantitate the extent of the potential defects in rearrangement in splenic samples from these mice, we utilized a real-time PCR assay with the degenerate VκD primer and a primer immediately downstream of Jκ1 (J1-2R) (Fig. 4*A* and *C*). This approach revealed that Vκ-Jκ1 rearrangement was 80% and 20% of WT levels in E3′−/− and DKO mice, respectively, whereas Ed−/− mice exhibited normal levels of recombination (Fig. 4*C*). To quantitate even more accurately the total extent of Vκ–Jκ rearrangements in DKO mice splenic B cells, we used Southern blotting after digestion with *EcoR*I and *BamH*I, and hybridization with an intronic Igκ gene probe, to evaluate the content of the 6.6 kb germline DNA band relative to tail and WT splenic B cell DNA controls, using the c-myb gene's hybridization signal to normalize the data (16,17) (Fig. 4*A* and *D*). The level of germline fragments was approximately 32% in splenic B cells from WT mice, and 64% from DKO mice corresponding samples (Fig. 4*D*). To complement further the above results, we also used real-time PCR to assay for the level of germline Igκ

sequences in splenic B cells from DKO, E3′−/−, Ed−/−, and WT mice, using KGL-F and KGL-R primers (Fig. 4A). As shown in Fig. 4*E*, the level of such germline sequences in DKO mice samples was about 70% of that of ES cell controls, while these levels were about 50% from E3′−/− mice, and approximately 35% from WT and Ed−/− mice. We also used a real-time PCR assay to evaluate rearrangement to the RS element in λ-producing splenic B cells from WT and mice of the other genotypes, using the degenerate VκD primer and primer RS101 (Fig. 4*A*). This assay revealed that Vκ-RS rearrangement was still readily detectable in DKO mice samples but severely compromised compared to the levels observed in samples from mice with the other genotypes (Fig. 4*F*).

One might imagine that the Igκ gene rearrangement observed in DKO splenic B cells may be occurring largely beyond the pre-B cell stage due to leakiness in recombinase specificity during and even after the assembly of the Igλ gene locus, perhaps even in later B cell developmental stages in the bone marrow and the periphery, leading to the accumulation of Igκ gene rearrangements in the background. To examine this possibility we took a step back in B cell development and performed real-time PCR assays for addressing the levels of locus germline retention and Vκ-Jκ1 rearrangement in isolated pre-B cells from mice of the various genotypes. As shown in Fig. 4*G* and *H*, germline retention was increased and Vκ-Jκ1 rearrangement was depressed in these samples compared to the levels seen in the corresponding samples from splenic B cells (compare Fig. 4*E* and *G*, or Fig. 4*C* and *H*). Most notably, rearrangement was most severely diminished in the pre-B cells from DKO mice. We conclude that although the combined presence of both E3′ and Ed are not absolutely required for Vκ gene rearrangement either to Jκ or RS elements, their presence together clearly maximizes the efficiencies of these rearrangement processes; furthermore, the rearrangement that occurs in the combined absence of these enhancers apparently is accumulating largely beyond the pre-B cell stage of development.

The steady-state levels of both rearranged and germline Igκ gene transcripts are vastly diminished in DKO mice B cells

Our results so far have revealed that Igκ gene expression at the level of cell surface protein is completely curtailed in splenic B cells yet such cells exhibit a low but very significant level of Vκ gene rearrangement. To address the effects of the DKO along with either E3′−/− or Ed−/− on the steady-state levels of spliced rearranged gene transcripts in splenic B cells, we utilized real-time RT-PCR to quantitate such transcript levels relative to WT controls. As shown in Fig. 5*A*, the level of transcripts arising from rearranged Igκ genes was reduced approximately 30-fold in DKO mice compared to those of WT, while those of E3′−/− or Ed −/− mice were 75% and 82% the levels of WT samples, respectively. We also assayed for the levels of spliced germline transcripts arising from the 5′ Igκ gene germline promoter (31) by real-time RT-PCR in pre-B cells from DKO mice and those from E3′−/− and Ed−/− mice relative to WT controls. As shown in Fig. 5*B*, the results of this analysis were very similar to those observed for rearranged gene transcripts, namely that DKO mice were essentially inactive in production of germline transcripts, whereas E3′−/− and Ed−/− mice were able to produce such transcripts at levels of approximately 60% of those seen in WT mice. We conclude that the DKO almost completely eliminates the ability of the Igκ gene to generate significant steady-state levels of spliced transcripts from either germline or rearranged genes.

DNA methylation is markedly increased in DKO Igκ genes

Previous studies have linked localized DNA methylation as contributing to silencing of immunoglobulin genes (for review, see ref. 32). Furthermore, both Ei and E3′ can promote a transcriptionally poised, undermethylated state at the Igκ locus (33). Therefore we investigated the effect of the DKO on the methylation status of several key CpG sites the Igκ

locus in pre-B cells. For this purpose, we selected CpG sites 1–6 for analysis specifically because several of these sites surround the KI and KII sequences known to be important for triggering gene rearrangement (34) (Fig. 6*A*); these sites will always be present in germline alleles but potentially become deleted or covalently rearranged in B cells. We also selected CpG sites 7–9 for analysis because these sites are essentially always present in Igκ alleles whether or not they have undergone V-J joining (Fig. 6*A*). As shown in Fig. 6*B*, with respect to sites 1–6, the Ed−/− mutation had only quantitative effects on altering methylation patterns relative to those of WT mice, but the E3′−/− mutation showed more significant effects at increasing methylation at most of CpG sites assayed for. However, sites 1–6 were found to be the most heavily methylated in DKO mice relative to the other controls, indicating that the two enhancers must work together to maximize undermethylation at these sites. By contrast, our analysis of sites 7–9 revealed that these sites were almost fully methylated in all genotypes of mice analyzed (Fig. 6*B*). In conclusion, the methylation status of the Igκ locus in DKO mice is characteristic of a silenced chromatin domain and is completely consistent with its dramatic shutdown in transcription.

Histone H3 acetylation is markedly reduced in the Jκ region of DKO mice pre-B cells

Previous studies have also linked numerous histone post-translational modifications to the activation or silencing of immunoglobulin genes (for reviews, see refs. 35,36). Furthermore, one hallmark modification for locus activation in pre-B cells is acetylation of histone H3 (AcH3) in the Jκ region (26). Therefore, to characterize further the epigenetic chromosomal state of the Igκ locus in DKO mice along with either E3′−/− or Ed−/− mice in pre-B cells relative to WT controls, we performed ChIP experiments with anti-AcH3 antibodies and utilized real-time RT-PCR to quantitate the results. As shown in Fig. 7, the Jκ1 and Jκ5 regions of WT mice were heavily enriched in their levels of AcH3 relative to the other lines of mice examined. However, AcH3 levels were most dramatically reduced in the Jκ1 and Jκ5 regions of DKO mice relative to the other controls, indicating that the two enhancers must work together to maximize this post-translational modification in the locus. In conclusion, the very low levels of AcH3 associated with the Igκ gene in DKO mice is a characteristic epigenetic signature of a silenced chromatin domain and is completely consistent with its enhanced DNA methylation and dramatic shutdown in transcription.

Discussion

We utilized BAC recombineering technology to create an ES cell targeting construct for generating DKO mice. This approach circumvents tedious conventional subcloning and PCR steps starting with λ phage libraries. In fact, in its ultimate form, state-of-the-art recombineering technology deserves special appreciation because it can generate ES cell targeting constructs with multiple mutations, using only PCR generated targeting cassettes, without even relying on restriction enzymes or DNA ligase (19,20,37). Furthermore, this technology avoids prolonged culturing of ES cells that accompanies repeated targeting strategies for the generation of multiple mutations, which can be problematic for achievement of eventual germline transmission of the desired mutations in subsequently generated chimeric mice. Although the Rag2−/− blastocyst complementation technique can be used in such instances to tease out phenotypes in chimeric animals (38), this approach is sometimes compromised because the number of cells arising from the ES cell donors can be variable and limiting.

We have found that the DKO mutation essentially eliminates Igκ gene expression, and results in the dominant expression of λ light chains. We also detected a significant block in B cell development in bone marrow, with a large increase in pre-B cells. This retardation in B cell development seen in bone marrow is entirely consistent with the known preferred order of light chain gene activation for rearrangement (1), and is also expected based on the

predominance of potentially functional Vκ genes normally available for recombination in WT mice, which far exceed by orders of magnitude potentially functional Vλ genes. This result is also reflected by a significant decrease in splenic $B220^+$ B cells in the periphery.

Germline transcription of the Igκ locus in pre-B cells has long been thought to increase locus accessibility to the recombinase apparatus and has been correlated with the process of Vκ-Jκ joining (23). Furthermore, deletion of the most 5′ Jκ-Cκ region germline promoter, which is known to be the most significant in pre-B cells for generating germline transcripts (31), is highly detrimental to Igκ gene rearrangement in knockout mice (39). These results are consistent with our observations of a marked inhibition seen in Igκ gene rearrangement in pre-B cells from DKO mice, which exhibited a ca. 50-fold decline in the steady-state level of germline transcripts arising from the 5′ germline promoter. Furthermore, we also found that in DKO pre-B cells the locus was essentially stoichiometrically methylated at several key CpG sites and deficient in AcH3 in the Jκ regions, conditions thought to be inhibitory to the process of gene rearrangement (26,32,35,36). Yet we detected significant levels of rearranged genes in the locus in splenic B cells of these mice. Thus, it is possible that although severely depressed, germline transcription triggered by the remaining enhancer Ei at the single-cell level may be high or at least above the minimum threshold required to transiently open chromatin accessibility to the recombination machinery during and after the pre-B cell stage of development. One experimentally well-supported model of enhancer action is probabilistic (40,41), in which enhancers affect the number of genes that get activated for transcription in a population of cells, and not the activity of the transcribing gene. Because DKO mice exhibit a retardation in development at the pre-B cell stage, short-duration pulses (42) of germline Igκ transcription may fluctuate from one-cell to the next during and even after the assembly of the Igλ gene locus, perhaps even in later B cell developmental stages in the bone marrow and the periphery, leading to the accumulation of Igκ gene rearrangements in the background. Such joining, although potentially functional as judged by the presence of abundant in-reading-frame junctions (data not shown), however, proved to be futile with respect to generation Igκ chains without the presence of either E3′ or Ed. We can therefore conclude from these results that E3′ and Ed play redundant roles in the locus for transcription and it is only when both enhancers are deleted can one visualize such a dramatic phenotype. We can further surmise further that Ei is not capable of driving significant transcription from the rearranged genes that exist in DKO splenic B cells.

The results of our studies taken together with those of other investigators also allow us to consider the relative developmental functions of the three Igκ gene enhancers in recombination. E3′−/− or Ed−/− mice still undergo Igκ gene recombination in pre-B cells at near WT levels, but recombination in DKO pre-B cells is severely hampered, and totally blocked in those of Ei−/− E3′−/− mice (18). Thus, in pre-B cells one can conclude that Ei must work together with either E3′ or Ed to foster recombination, probably by a looping mechanism for activating transcription from the 5′ germline promoter. In addition, Ei but not E3′ or Ed is required for the earlier and more efficient rearrangement of κ vs λ loci during B cell development (15–17), and for allowing efficient secondary Vκ gene rearrangements to the downstream Jκ regions (18).

We have previously noted that Ed forms a DNase I hypersensitive site in B cell chromatin in plasmacytoma but not pre-B cell lines (9), an observation also consistent with a functional role for Ed later in B cell maturation. However, in earlier studies we found that there was no difference in plasma cell number between WT and Ed−/− mice (17). In the current study we can deduce from our results unexpected compensatory roles for Ed in E3′−/− mice in triggering germline transcription, and Vκ gene rearrangements to both Jκ and RS elements. For example, because in Ed−/− mice there is no defect in recombination (17), whereas in DKO mice the observed defects in recombination far exceed those seen in E3′−/− mice, we

can conclude that Ed must play a compensatory role in Igκ gene recombination events in E3′ −/− mice. Thus it appears that under conditions where E3′ is absent, the locus switches the normal developmental timing of Ed activation to an earlier stage.

Our previous studies have shown that the Ed enhancer synergistically activates transcription in combination with other enhancers, like Ei (9), and that Ed forms complexes with Ei and E3′ with the looping out of the intervening DNA in stimulated splenic B cells as well as plasmacytoma cell lines (13,14). Taken together with the results of the present investigation, it seems clear that E3′ and Ed must work together to optimally set up active chromatin loop domains and to drive high level Igκ gene germline transcription in pre-B cells and high level rearranged gene transcription in both resting and activated B cell states.

In conclusion, our results together with other published studies on endogenous Igκ locus enhancer knockout mice have permitted us to functionally delineate the roles that the three Igκ gene enhancers play developmentally in triggering rearrangement and transcription. We can conclude that E3′ and Ed have redundant functions in the locus and have uncovered a compensatory developmental switch in Ed when E3′ is missing from the locus.

Supplementary Material

Refer to Web version on PubMed Central for supplementary material.

Acknowledgments

We thank Mark Schlissel for providing mice, Xiaoling Ding for expert technical support and Jose Cabrera for graphic illustrations. We are indebted to Nicolai van Oers for his insightful comments and suggestions.

This investigation was supported by Grants GM29935 and AI067906 from the National Institutes of Health and Grant I-0823 from the Robert A. Welch Foundation to WTG.

Abbreviation

E3′	3′ enhancer
Ed	downstream enhancer
DKO	homozygous E3′-Ed double knockout
RS	recombination sequence
ChIP	chromatin immunoprecipitation

References

1. Yancopoulos GD, Alt FW. Developmental controlled and tissue-specific expression of unrearranged VH gene segments. Cell. 1985; 40:271–281. [PubMed: 2578321]
2. Brekke KM, Garrard WT. Assembly and analysis of the mouse immunoglobulin kappa gene sequence. Immunogenetics. 2004; 56:490–505. [PubMed: 15378297]
3. Gellert M. Recombination: RAG proteins, repair factors, and regulation. Ann. Rev. Biochem. 2002; 71:101–132. [PubMed: 12045092]
4. Schlissel MS. Regulation of activation and recombination of the murine Igκ locus. Immunol. Rev. 2004; 200:215–223. [PubMed: 15242407]
5. Durdik JM, Moore MW, Selsing E. Novel κ light chain rearrangements in mouse λ light chain producing B lymphocytes. Nature. 1984; 307:749–750. [PubMed: 6422305]
6. Nadel B, Cazenave PA, Sanchez P. Murine lambda gene rearrangements: the stochastic model prevails over the ordered model. EMBO J. 1990; 9:435. [PubMed: 2105884]

7. Shimizu T, Iwasato T, Yamagishi H. Deletions of immunoglobulin Cκ region characterized by circular excision products in mouse splenocytes. J. Exp. Med. 1991; 173:1065–1072. [PubMed: 1902500]
8. Vela JL, Aït-Azzouzene D, Duong BH, Ota T, Nemazee D. Rearrangement of mouse immunoglobulin kappa deleting element recombining sequence promotes immune tolerance and lambda cell production. Cell. 2008; 28:161–170.
9. Liu ZM, George-Raizen JB, Li S, Meyers KC, Chang MY, Garrard WT. Chromatin structural analyses of the mouse Igκ gene locus reveal new hypersensitive sites specifying a transcriptional silencer and enhancer. J. Biol. Chem. 2002; 277:32640–32649. [PubMed: 12080064]
10. Queen C, Baltimore D. Immunoglobulin gene transcription is activated by downstream sequence elements. Cell. 1983; 33:741–748. [PubMed: 6409419]
11. Xu M, Barnard MB, Rose SM, Cockerill PN, Huang S-Y, Garrard WT. Transcription termination and chromatin structure of the active immunoglobulin κ gene locus. J. Biol Chem. 1986; 261:3838–3845. [PubMed: 3081510]
12. Meyer KB, Neuberger MS. The immunoglobulin κ locus contains a second, stronger B cell specific enhancer which is located downstream of the constant region. EMBO J. 1989; 8:1959–1964. [PubMed: 2507312]
13. Liu Z, Garrard WT. Long range interactions between three transcriptional enhancers, active Vκ gene promoters and a 3' boundary sequence spanning 46 kb. Mol. Cell. Biol. 2005; 25:3220–3231. [PubMed: 15798207]
14. Liu Z, Ma Z, Terada LS, Garrard WT. Divergent roles of RelA and c-Rel in establishing chromosomal loops upon activation of the Igκ gene. J. Immunol. 2009; 183:3819–3830. [PubMed: 19710460]
15. Xu Y, Davidson L, Alt FW, Baltimore D. Deletion of the Igκ light chain intronic enhancer/matix attachment region impairs but does not abolish Vκ-Jκ rearrangement. Immunity. 1996; 4:377–385. [PubMed: 8612132]
16. Gorman JR, Van der Stoep N, Monroe R, Cogne M, Davidson L, Alt FW. The Igκ 3′ enhancer influences the ratio of Ig(kappa) versus Ig(lambda) B lymphocytes. Immunity. 1996; 5:241–252. [PubMed: 8808679]
17. Xiang Y, Garrard WT. The downstream transcriptional enhancer, Ed, positively regulates mouse Igκ gene expression and somatic hypermutation. J. Immunol. 2008; 180:6725–6732. [PubMed: 18453592]
18. Inlay M, Alt FW, Baltimore D, Xu Y. Essential roles of the κ light chain intronic enhancer and 3' enhancer in κ rearrangement and demethylation. Nat. Immunol. 2002; 3:463–468. [PubMed: 11967540]
19. Liu P, Jenkins NA, Copeland NG. A highly efficient recombineering-based method for generating conditional knockout mutations. Genome Res. 2003; 13:476–484. [PubMed: 12618378]
20. Chan W, Costantino N, Li R, Lee SC, Su Q, Melvin D, Court DL, Liu P. A recombineering based approach for high-throughput conditional knockout targeting vector construction. Nucleic Acids Res. 2007; 35:e64. [PubMed: 17426124]
21. Tallquist MD, Soriano P. Epiblast-restricted Cre expression in MORE mice: a tool to distinguish embryonic vs. extra-embryonic gene function. Genesis. 2000; 26:113–115. [PubMed: 10686601]
22. Farley FW, Soriano P, Steffen LS, Dymecki SM. Widespread recombinase expression using FLPeR (Flipper) mice. Genesis. 2000; 28:106–110. [PubMed: 11105051]
23. Schlissel MS, Baltimore D. Activation of immunoglobulin κ gene rearrangement correlates with induction of germline κ gene-transcription. Cell. 1989; 58:1001–1007. [PubMed: 2505932]
24. Inlay MA, Lin T, Gao HH, Xu Y. Critical roles of the immunoglobulin intronic enhancers in maintaining the sequential rearrangement of IgH and Igκ loci. J. Exp. Med. 2006; 203:1721–1732. [PubMed: 16785310]
25. Retter MW, Nemazee D. Receptor editing occurs frequently during normal B cell development. J. Exp. Med. 1998; 188:1231–1238. [PubMed: 9763602]
26. Xu C-R, Feeney AJ. The epigenetic profile of Ig genes is dynamically regulated during B cell differentiation and is modulated by pre-B cell receptor signaling. J. Immunol. 2009; 182:1362–1369. [PubMed: 19155482]

27. Rolink A, Grawunder U, Winkler TH, Karasuyama H, Melchers F. IL-2 receptor alpha chain (CD25, TAC) expression defines a crucial stage in pre-B cell development. Int. Immunol. 1994; 6:1257–1264. [PubMed: 7526894]
28. Hardy RR, Carmack CE, Shinton SA, Kemp JD, Hayakawa K. Resolution and characterization of pro-B and pre-pro-B cell stages in normal mouse bone marrow. J. Exp. Med. 1991; 173:1213–1225. [PubMed: 1827140]
29. Hewitt SI, Yin D, Ji Y, Chaumeil J, Marszalek K, Tenthorey J, Salvagiotto G, Steinel N, Ramsey LB, Ghysdael J, Farrar MA, Sleckman BP, Schatz DG, Busslinger M, Bassing CH, Skok JA. RAG-1 and ATM coordinate monoallelic recombination and nuclear positioning of immunoglobulin loci. Nature Immunol. 2009; 10:655–664. [PubMed: 19448632]
30. Ma S, Pathak S, Mandal M, Trinh L, Clark MR, Lu R. Ikaros and aiolos inhibit pre-B cell proliferation by directly suppressing c-myc expression. Mol. Cell. Biol. 2010; 30:4149–4158. [PubMed: 20566697]
31. Amin RH, Cado D, Nolla H, Huang D, Shinton SA, Zhou Y, Hardy RR, Schlissel MS. Biallelic, ubiquitous transcription from the distal germline Igκ locus promoter during B cell development. Proc. Natl. Acad. Sci. USA. 2009; 106:522–527. [PubMed: 19116268]
32. Mostoslavsky R, Berman Y. DNA methylation: Regulation of gene expression and role in immune system. Biochim. Biophys. Acta. 1997; 1333:F29–F50. [PubMed: 9294017]
33. Mostoslavsky R, Singh N, Kirillov A, Pelanda R, Cedar H, Chess A, Berman Y. κ chain monoallelic demethylation and the establishment of allelic exclusion. Genes Dev. 1998; 12:1801–1811. [PubMed: 9637682]
34. Ferradini L, Gu H, Smet AD, Rajewsky K, Reynaud C-A, Weill J-C. Rearrangement-enhancing element upstream of the mouse immunoglobulin kappa chain J cluster. Science. 1996; 271:1416–1420. [PubMed: 8596914]
35. Schlissel MS, Schulz D, Vetterman C. A histone code for regulating V(D)J recombination. Mol. Cell. 2009; 34:639–640. [PubMed: 19560416]
36. Degner-Leisso SC, Feeney AJ. Epigenetic and 3-dimensional regulation of V(D)J rearrangement of immunoglobulin genes. Semin. Immunol. 2010; 22 In Press.
37. Testa G, Vintersten K, Zhang Y, Benes V, Muyrers JPP, Stewart AF. BAC engineering for the generation of ES cell-targeting constructs and mouse transgenes. Methods Molec. Biol. 2004; 256:123–139. [PubMed: 15024164]
38. Chen J, Lansford R, Stewart V, Young F, Alt F. RAG-2-deficient blastocyst complementation: an assay of gene function in lymphocyte development. Proc. Natl. Acad. Sci. USA. 1993; 90:4528–4532. [PubMed: 8506294]
39. Cocea L, DeSmet A, Saghatchian M, Fillatreau S, Ferradini L, Schurmans S, Weill J-C, Reynaud C-A. A targeted deletion of a region upstream from the Jκ cluster impairs κ chain rearrangement in cis in mice and in the 103/bcl2 cell line. J. Exp. Med. 1999; 189:1443–1449. [PubMed: 10224284]
40. Walters MC, Fiering S, Eidemiller J, Magis W, Groudine M, Martin DI. Enhancers increase the probability but not the level of gene expression. Proc. Natl. Acad. Sci. USA. 1995; 92:7125–7129. [PubMed: 7624382]
41. Sen R, Grosschedl R. Memories of lost enhancers. Genes Dev. 2010; 24:973–979. [PubMed: 20478992]
42. Larson DR, Singer RH, Zenklusen D. A single molecule view of gene expression. Trends Cell Biol. 2009; 19:630–637. [PubMed: 19819144]

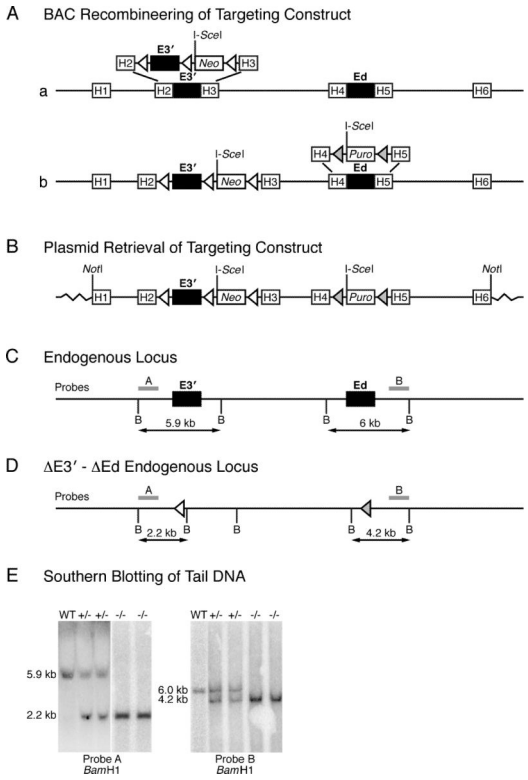

FIGURE 1.

Production of the DKO targeting construct by BAC recombineering and subsequent creation of knockout mice. *A*, BAC recombineering of the targeting construct. *a*, Relevant segment of the Igκ locus in a BAC, with open boxes H1-H6 indicating homologous sequences used for various targeting steps and the closed rectangles depicting the enhancers. Sequences bearing loxP sites and a *Neo* gene were introduced flanking E3′ through homologous sequences H2 and H3. *b*, Ed was next replaced with a *Puro* cassette flanked by frt sites through homologous sequences H4 and H5. *B*, plasmid pL611 (wavy lines) with homologous ends H1 and H6 were used to retrieve the engineered Igκ gene region from the BAC to make the DKO targeting construct. *C*, Structure of the native endogenous locus, with the positions of hybridization probes A and B indicated together with the sizes of their *Bam*H1(B)-cleaved, genomic-DNA-hybridizing-products. *D*, Structure of the targeted endogenous locus after deletion of the *Neo* and *Puro* targeted regions by Cre and Flp recombinases, with probes and hybridizing cleavage products indicated as above. The positions of the single remaining loxP and frt sites are depicted by open and shaded triangles, respectively. *E*, Southern blotting of tail DNA, after digestion with *Bam*H1 and hybridization with probe A or probe B. A 5.9 kb band derived from the WT allele and a 2.2 kb band derived from the E3′-deleted-allele were detected by Probe A. A 6.0 kb band derived from the WT allele and a 4.2 kb band derived from the Ed-deleted-allele were detected by probe B.

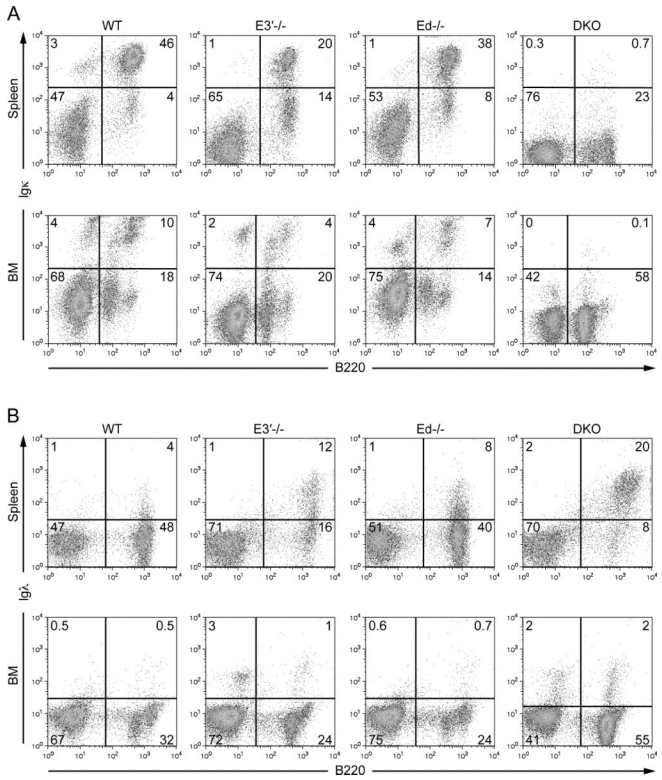

FIGURE 2.

FACS analysis of surface Ig expression in spleen and bone marrow reveals that DKO mice cannot generate Igκ expressing B cells. Data are representative of at least three independent experiments. *A*, Analysis of Igκ$^+$ B cells in spleen and bone marrow (BM) of WT, E3′−/−, Ed−/−, and DKO mice. B, Analysis of Igλ$^+$ B cells in spleen and bone marrow (BM) of WT, E3′−/−, Ed−/−, and DKO mice.

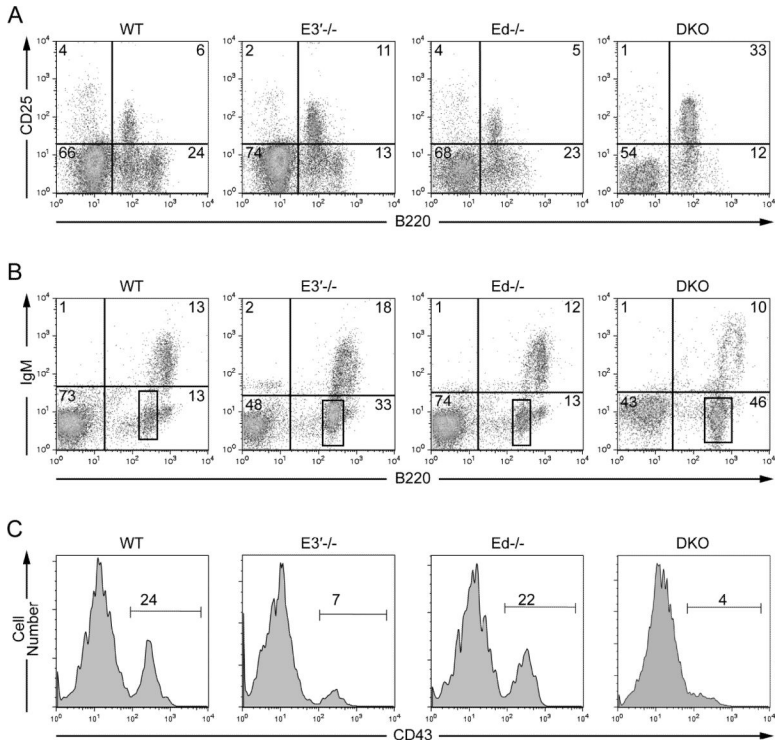

FIGURE 3.

FACS analysis of bone marrow cells reveals that early B cell development in DKO mice is significantly arrested at the pre-B cell stage. Data are representative of at least three independent experiments. A, Analysis of pre-B cells in bone marrow of WT, E3′−/−, Ed−/−, and DKO mice using CD25 as a pre-B cell marker (27). *B*, Bone marrow cells were FACS-analyzed with respect to B220 and IgM markers. The $B220^{low}IgM^{-}$ cells were gated for each genotype as indicated by the rectangles and their CD43 expression was analyzed in Panel C. The percentages of pro-B cells ($B220^{low}IgM^{-}CD43^{+}$) are indicated by the horizontal bars (28).

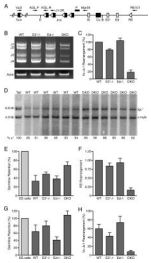

FIGURE 4.

The absence of the two enhancers decreases Igκ locus gene rearrangement. *A*, The schematic depicts the positions in the Igκ locus (not to scale) of the degenerate VκD primer and other indicated primers used in various PCR assays (arrows). Vκ, Jκ, and Cκ exons are closed rectangles, Ei, E3′, and Ed enhancers are open rectangles, and RSS or RS elements are open triangles. *Eco*RI (E) and *BamH*I (B) cutting sites are indicated and the position of the Southern blot hybridization probe (P, horizontal solid bar). *B*, Results of the PCR assay used to evaluate J-region usage of Igκ rearrangements in splenic $B220^+$ B cells using the VκD and Mar35 primers. Data shown are representative of at least three independent experiments. *C*, Results of the real-time PCR assay used to measure the levels of Vκ-Jκ1 rearrangement in $B220^+$ splenic B cells using the VκD and J1-2R primers. Data are presented as means ± SD (n=3), normalized to the corresponding rearrangement level seen in WT splenic $B220^+$ samples taken as 100%. *D*, Southern blotting of tail DNA and $B220^+$ splenic cell DNA isolated from individual WT and DKO mice as indicated, after digestion with *Eco*RI and *Bam*HI and hybridization with an intronic Igκ and c-myb probes. The amount of the 6.6 kb Igκ germline DNA signal was normalized by the 4.3 kb c-myb signal as follows. Igκ germline (κ°)/c-myb ratio in mouse tail DNA was set as 100%. The % κ° for each sample were calculated as: [(κ°/c-myb in samples)/(κ°/c-myb in tail DNA)] × 100%. *E*, Results of the real-time PCR assay used to detect germline retention of Igκ sequences in splenic $B220^+$ B cells using the KGL-F and KGL-R primers. The percentage of germline retention was calculated by dividing the germline sequence levels of B cells by those of ES cells. Data are presented as means ± SD (n=3). (DKO vs WT, $p<0.01$, E3′−/− vs WT, $p=0.06$). *F*, Results of the real-time PCR assay used to measure the levels of RS rearrangement in splenic λ-expressing B cells using the VκD and RS101 primers. Data are presented as means ± SD (n=3). (DKO vs WT, $p<0.01$). *G*, Results of the real-time PCR assay used to detect germline retention of Igκ sequences in bone marrow pre-B cells using the KGL-F and KGL-R primers. The percentage of germline retention was calculated by dividing the germline sequence levels of B cells by those of ES cells. Data are presented as means ± SD (n=3–6). (DKO vs WT, $p<0.001$, Ed−/− vs WT, $p=0.04$). *H*, Results of the real-time PCR assay used to measure the levels of Vκ-Jκ1 rearrangement in bone marrow pre-B cells using the VκD and J1-2R primers. Data are presented as means ± SD (n=3), normalized to the corresponding rearrangement level seen in WT splenic $B220^+$ samples taken as 100%. (DKO vs WT, $p<0.001$; E3′−/− vs WT, $p=0.03$).

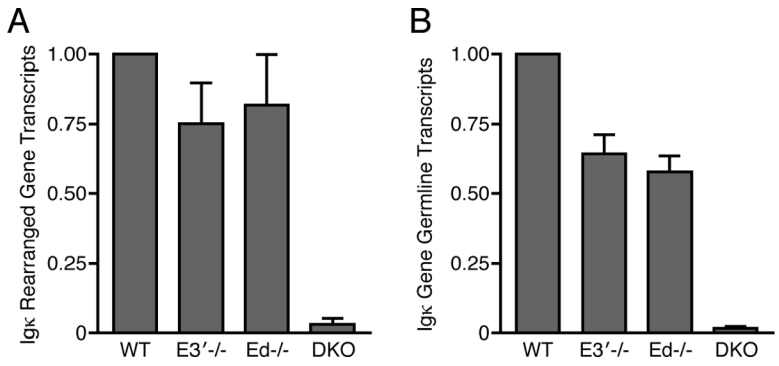

FIGURE 5.

Igκ gene transcription is nearly completely abolished in DKO mice spleen and bone marrow. *A*. The results of a real-time PCR assay used to measure rearranged Igκ gene transcription in splenic B cells. Data are presented as means ± SD (n=3) (DKO vs WT, $p<0.01$; E3′−/− vs WT, $p=0.07$; Ed−/− vs WT, $p=0.24$; E3′−/− vs Ed−/−, $p=0.48$; E3′−/− or Ed−/− vs DKO, $p<0.01$). *B*. The results of a real-time PCR assay used to measure Igκ gene germline transcription in pre-B cells initiated from the 5′ promoter. Data are presented as means ± SD (n=3) (E3′−/− or Ed−/− or DKO vs WT, $p<0.01$; E3′−/− vs Ed−/−, $p=0.11$, E3′−/− or Ed−/− vs DKO, $p<0.01$).

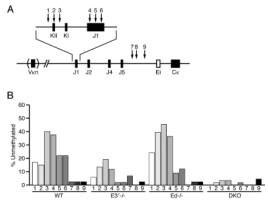

FIGURE 6.

Methylation in the Igκ locus is greatly increased in DKO pre-B cells at multiple CpG sites. *A.* The methylation status of nine CpG sites were analyzed by the bisulfite method in pre-B cells from bone marrow as indicated in the schematic. *B.* Results presented represent the means from at least thirty individual sequenced clones from each mice group.

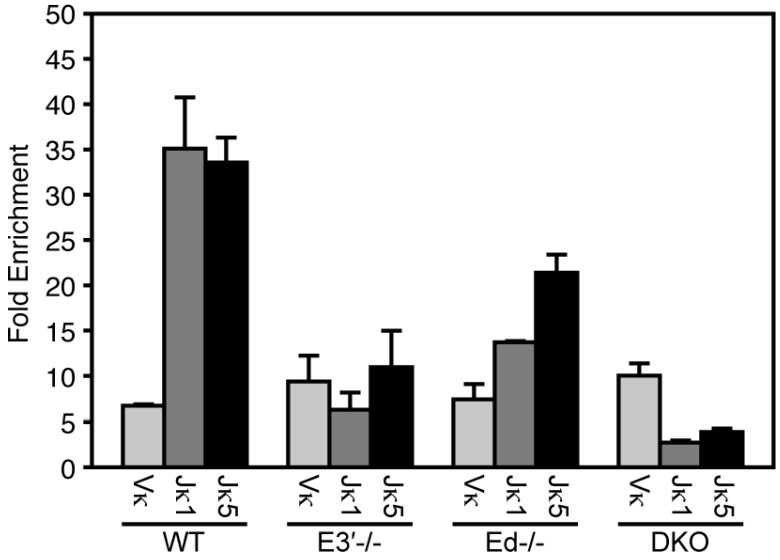

FIGURE 7.

Histone H3 acetylation is abolished in Jκ regions of DKO pre-B cells. Real time PCR ChIP assays of AcH3 levels in pre-B cells of the indicated mice strains. Fold enrichment refers to the sequence abundance in the immunoprecipitated sample divided by the corresponding sequence abundance in input DNA relative to a control GAPDH gene. Data are presented as means ± SD (n=2). For Jκ1 or Jκ5 AcH3 levels (DKO vs WT, $p<0.01$; E3′−/− vs WT, $p=0.02$; Ed−/− vs WT, $p=0.04$). There are no statistically significant differences for Vκ AcH3 levels between the different mice lines.

TABLE I

Primers for PCR and RT-PCR assays.

Southern probe A	5′-taatagagaatgaggcttaaggcagggctata-3′ 5′-gcttccggaatcagcaaccatacacaagagctag-3′
Southern probe B	5′-agtacagatgtgtaaaataaactgcaaaa-3′ 5′-cgcagatactctaccacttgcttttaacaa-3′
Degenerate Vκ primer (VκD)	5′-ggctgcagsttcagtggcagtggrtcwggrac-3′
Mar35	5′-acactggataaagcagtttatgccctttc-3′
J1-2R	5′-gacaacggaagaaagagactttgga-3′
KGL-F	5′-agctacccactgctctgttc-3′
KGL-R	5′-cgtttgatttccagcttggt-3′
RS101	5′-acatggaagttttcctgggagaatat-3′
KGT-F	5′-gcacacttagctctcatttcccaccccag-3′
KGT-R	5′-atgaactagaaattaatattgtttgtctg-3′
Cκ primer	5′-aggacgccattttgtcgttcact-3′